Development and evaluation of a thermodynamic dataset for phases of interest in CO_2 mineral sequestration in basaltic rocks

E.S.P. Aradóttir[a,b,*], E.L. Sonnenthal[c], H. Jónsson[a]

[a] *Science Institute, University of Iceland, Dunhaga 3, 107 Reykjavík, Iceland*
[b] *Reykjavík Energy, Baejarhálsi 1, 110 Reykjavík, Iceland*
[c] *Lawrence Berkeley National Laboratory, 1 Cyclotron Rd, Berkeley CA 94720, USA*

Abstract

A thermodynamic dataset describing 36 mineral reactions of interest for CO_2-water-basalt interaction associated with CO_2 mineral sequestration in basaltic formations is presented. Mineral selection for the dataset is based on extensive review of natural analogs of water-basalt interaction at low and elevated CO_2 conditions. Widely used thermodynamic databases did not contain the mineral assemblage needed for successfully simulating the alteration processes observed in nature as important primary and secondary minerals were found to be missing.

The EQ3/6 V7.2b database is the primary source for aqueous equilibrium constants in the developed dataset but reactions for four missing Al-hydroxy complexes were added. Recently published thermodynamic data were compiled for most of the minerals considered in this study. Mineral solubility constants obtained directly from measurements were compiled to the dataset without modification but SUPCRT was used for computing solubility constants when such data was not available.

In order to verify that the presented dataset can capture alterations observed in nature, simulations of CO_2-water-basalt interaction were carried out at low and elevated CO_2 conditions and compared to observed basalt alteration in Iceland and Greenland. Overall simulated and observed alteration are in good agreement, both at low and elevated CO_2 conditions, suggest-

*Corresponding author. *Address*: Reykjavík Energy, Baejarhálsi 1, 110, Reykjavík, Iceland. *Tel*: +354 516 6992. *Fax*: +354 516 6709

Email address: edda.sif.aradottir@or.is (E.S.P. Aradóttir)

ing the dataset to be well suited for simulations of e.g. CO_2-water-basalt interaction associated with CO_2 mineral sequestration in basalts.

Keywords: Thermodynamic dataset, CO_2-water-basalt interaction, geochemical modeling, CO_2 geological storage, *in situ* CO_2 mineral sequestration

1. Introduction

Great advances have been made in geochemical computer simulations in recent decades. The creation and compilation of thermodynamic databases, along with improved computer technology, laid the basis for this development. The databases have been used with geochemical computer codes, such as EQ3/6 (Wolery, 1983, 1992), WATCH (Arnórsson et al., 1982; Bjarnason, 1994), SUPCRT92 (Johnson et al., 1992), PHREEQC (Parkhurst et al., 1980; Parkhurst and Appelo, 1999) and TOUGHREACT (Xu et al., 2006, 2011), allowing for rapid simulations of mineral solubility and solute speciation in a variety of geochemical systems. The codes differ in complexity and ease of use, but all accurately solve for the equilibrium assemblages of minerals and aqueous species, and mineral solubilities within the limits of their thermodynamic databases. The quality of the results obtained is directly related to the quality of the databases used (Oelkers et al., 2009).

Among currently widely used databases are the SUPCRT databases, the EQ3/6 database, the LLNL thermochemical database (Delaney and Wolery, 1989) and THERMODDEM (Blanc et al., 2009), which specifically focuses on nuclear waste systems. The SOLTHERM database developed by Reed and Palandri (2006a) has also been substantially used in numerical simulations of hydrothermal processes. LLNL and THERMODDEM are both based on the EQ3/6 database, which in turn is originally based on the SUPCRT database. SOLTHERM is to a large degree based on the database of Holland and Powell (1998) and SLOP.98 (Shock et al., 1997; Plyasunova et al., 2004), the modified SUPCRT database (Reed and Palandri, 2006b). Many minerals and species thus have similar properties in different databases while major differences can occur for several minerals (e.g. Engi, 1992).

Government and industry rely increasingly on the results of model calculations when addressing critical societal problems, such as nuclear waste storage and remediation of toxic waste plumes (Oelkers et al., 2009; Spycher et al., 2007; Steefel et al., 2005). CO_2 capture and sequestration projects also

use model calculations extensively in order to predict the long-term fate of sequestered CO_2 and identify potential environmental effects, as emphasized in the EU directive on geological CO_2 storage (EU, 2009). As quality of modeling results is e.g. directly related to the quality of the thermodynamic database used, compilation and evaluation of the databases is a necessary step in all geochemical modeling work.

Even though widely used databases often provide excellent predictions when used in numerical modeling, they commonly lack important minerals for specific modeling tasks. Furthermore, they may not contain new and/or improved data that is continuously being published. Standard databases should, therefore, be thought of as being a work in progress rather than a completed task.

This paper presents a thermodynamic dataset describing 36 mineral reactions of interest for CO_2-water-basalt interaction. Mineral selection for the dataset is based on extensive review of natural analogs of water-basalt interaction at low and elevated CO_2 conditions. Compilation of the dataset is a part of modeling activities carried out with the objective of developing multidimensional field scale reactive transport models of CO_2 mineral sequestration in Icelandic basalts (see Aradóttir et al., 2011; Aradóttir, 2011, and references therein for more detail). TOUGHREACT is used for the model development and therefore thermodynamic data is published in TOUGHREACT-style, i.e. log K values are provided at eight different temperature (0, 25, 60, 100, 150, 200, 250 and 300 °C). These temperature values are commonly used by other computer codes as well, e.g. the EQ3/6 code. Equilibrium constants can be incorporated in the thermodynamic databases of these codes without further modification, provided that the databases used are set up with respect to the basis set of aqueous species as used in this study.

2. Natural analogs of CO_2-water-basalt interaction

Natural analogs of CO_2-water-basalt interaction provide important insight into the alteration mineralogy associated with CO_2 mineral sequestration. Natural analogs from Iceland and Greenland were used to identify primary and secondary minerals that are likely to be involved in CO_2 geological storage in basaltic rocks. Basalt compositions can range from 100% glass to 100% crystalline (Gudbrandsson et al., 2011). Crystalline glass consists predominantly of olivine, plagioclase and pyroxene but to a lesser degree of Fe-Ti oxides and sometimes also apatite.

Basalt weathering and alteration in low temperature (<100°C) geothermal fields in Iceland result from interaction of primary rocks with low CO_2 waters of meteoric origin (Rogers et al., 2006). Secondary minerals commonly associated with basalt weathering by CO_2 depleted waters are amorphous or poorly crystalline hydroxides, allophane, imogolite, kaolinite and clay minerals such as Mg, Ca, and Fe rich smectites (Crovisier et al., 1992; Arnalds, 1990; Wada et al., 1992; Arnalds et al., 1995; Stefánsson and Gíslason, 2001). Alteration mineralogy in low temperature geothermal fields in Iceland has e.g. been obtained by studying alteration products of fossil systems, mainly in East Iceland (Walker, 1960; Neuhoff et al., 1999), and from well drill cuttings (Kristmannsdóttir and Tómasson, 1978). These studies indicate alteration products to be dominated by clay minerals and zeolites, calcite and amorphous silica, quartz and/or chalcedony. Similar studies have been carried out for the Hengill high-temperature system showing mineral assemblages formed at higher temperature (Helgadóttir et al., 2010; Franzson et al., 2010; Níelsson, 2011). Smectites, celadonite and chlorites are the most commonly found clay minerals in association with hydrothermal basalt alteration in Iceland. Commonly found zeolites include analcime, chabazite, thomsonite, scolecite, phillipsite, mesolite, stilbite, stellerite and heulandite.

Rogers et al. (2006) reported results of basalt alteration under elevated CO_2 conditions in Marraat at Nuussuaq, W-Greenland. There, alteration of basalts formed regionally extensive, silica-deficient zeolite-facies mineral assemblages that dominantly consist of mixed-layer chlorite/smectite clays, thomsonite, natrolite, gonnardite, analcime and chabazite. In the study area, faulting and fracturing allowed for petroleum migration from sediments into the overlying basalts. Migration of petroleum and the associated brine led to the pseudomorphic replacement of zeolite and clay mineral assemblages with carbonates (siderite, magnesite, dolomite and calcite) and quartz at temperature of ∼80-125° C. Carbonates associated with the petroleum migration are rich in Mg and Fe, reflecting the interaction of a CO_2 rich fluid with a picritic (i.e. Mg- and Fe-rich) basalt. Only late stage carbonates in Marraat are calcium rich, the result of depletion of aqueous magnesium and iron following precipitation of magnesite-siderite solid solutions.

Table 1 gives a summary on secondary minerals commonly found in association with basalt alteration.

3. Compatibility of widely used thermodynamic databases

Mineral assemblages compiled to the EQ3/6, LLNL, THERMODDEM and SOLTHERM thermodynamic databases were reviewed with respect to the minerals needed to simulate natural alteration processes associated with CO_2-water-basalt interaction at low and elevated CO_2 conditions.

All the databases lack basaltic glass as well as the primary crystalline minerals observed in Icelandic basalts, i.e. plagioclase, pyroxene and olivine. The databases do, however, contain individual end-member minerals for the crystalline minerals but these will not provide sufficiently good description of primary basaltic rock in Iceland as the chemical compositions of plagioclase and pyroxene in particular are far from end-member compositions (see e.g. Gudbrandsson et al., 2011).

Important secondary minerals are also missing from the databases. EQ3/6 does not contain various Ca and Na zeolite end-members, which are important for capturing observed zeolite formations in numerical simulations. Different celadonite and chlorite end-members are missing from the LLNL database along with some important zeolites (e.g. chabazite and heulandite). THERMODDEM is missing some zeolites, hydroxides as well as important clay minerals and other silicates. The SOLTHERM database lacks many of the zeolites and hydroxides observed in natural analogs of CO_2-water-basalt interaction.

As important minerals are missing from all the reviewed databases, none of them was found to contain the mineral assemblage necessary for successfully simulating CO_2-water-basalt interaction at low and elevated CO_2 conditions. As a result, a database containing the required mineral assemblage was developed.

4. Minerals and species in developed dataset

Table 2 summarizes the chemical composition of the minerals considered in this study. The mineral selection is based on the natural analogs of CO_2 rich and depleted water-basalt interaction discussed above.

Minerals are listed under the headings primary basaltic minerals and glasses, silicates, hydroxides, carbonates and zeolites. Aqueous species are listed separately. Dissolution reactions for the minerals considered in the present study are shown in table 3. All mineral dissolution reactions are written in terms of the same basis species set (H_2O, H^+, HCO_3^-, $Al(OH)_4^-$,

Fe^{2+}, Mg^{2+}, Na^{+}, K^{+}, $SiO_{2\,(aq)}$, Cl^{-} and $O_{2\,(aq)}$). Selection of basis species is primarily based on the findings of Stefánsson et al. (2001), who studied dominant aqueous species in natural waters in the basaltic terrain of Iceland. All other species and minerals in the dataset, are written in terms of the basis species. The number of secondary species and minerals must be equal to the number of independent reactions. Any of the secondary species can be represented as a linear combination of the set of basis species.

4.1. Aqueous species

The EQ3/6 V7.2b database (Wolery, 1992) is the primary source for aqueous equilibrium constants used in this study. Four Al-hydroxy complexes were, however, added to the dataset; $AlOH^{2+}$, $Al(OH)_2^{+}$, $Al(OH)_3$ and $Al(OH)_4^{-}$. As discussed by Arnórsson (1999), the dominant Al-hydroxy species in many natural waters is $Al(OH)_4^{-}$, which is why it was selected as a primary species.

4.2. Primary minerals and glasses

Four primary minerals and glasses are considered in this study: Plagioclase, pyroxene, olivine and basaltic glass. Fe-Ti oxides (titanomagnetite and ilmenite) and apatite are also common primary minerals in Icelandic basalts. These were, however, not included in the study due to their low abundance and significantly lower reactivity as discussed in more detail in section 9.

Basaltic glass

Basaltic glass from Stapafell, SW Iceland, was selected as a representative for the glass phase. This was done, as the Stapafell glass has been extensively studied especially with respect to dissolution kinetics (e.g. Oelkers and Gíslason, 2001; Gíslason and Oelkers, 2003).

Crystalline basalt – Olivine, plagioclase and pyroxene

Primary minerals of crystalline basalt, which in the current study include olivine, plagioclase and pyroxene, all form solid solutions between two or more end-members. Olivine and plagioclase form binary solid solutions between forsterite (Fo, Mg_2SiO_4) and fayalite (Fa, Fe_2SiO_4) and anorthite (An, $CaAl_2Si_2O_8$) and albite (Ab, $NaAlSi_3O_8$), respectively. The pyroxene considered here is augite, a quaternary solid solution between enstatite (En, $MgSiO_3$), ferrosilite (Fe, $FeSiO_3$), diopside (Di, $Mg_{0.5}Ca_{0.5}SiO_3$) and hedenbergite (Hd, $Fe_{0.5}Ca_{0.5}SiO_3$). The specific composition of the solid solutions

were those given by Stefánsson (2001). The compositions are $Fo_{80}Fa_{20}$ for olivine, $Di_{45}Hd_{25}En_{19}Fs_{11}$ for pyroxene and $An_{70}Ab_{30}$ for plagioclase.

4.3. Secondary minerals

32 secondary minerals are considered in this study. They are all known to form in basalt weathering and alteration.

Silicates

Among clay minerals, smectites, celadonite and chlorite are all commonly formed in basalt alteration in Iceland. Montmorillonite was selected as a representative for smectites and allowed to precipitate as a solid solution between Ca, K, Mg and Na end-members. Celadonite also forms solid solutions between Fe and Mg end-members. Clinochlore and daphnite from Holland and Powell (1998) were chosen as Mg- and Fe-rich chlorite end-members in a precipitating solid solution.

Other common silicate weathering and alteration minerals in basalts considered in this study include allophane, imogolite, kaolinite, antigorite, amorphous silica, moganite and quartz. Moganite is a silicate mineral with the chemical formula SiO_2 that was initially described by Flörke et al. (1976). Moganite is considered a polymorph of quartz: it has the same chemical composition as quartz, but a different crystal structure. A growing body of evidence reveals that much of the silica that crystallizes at the Earth's surface is a finely intergrown mixture of quartz and moganite. Chalcedony, for example is made up of both moganite and quartz (Gíslason et al., 1997).

Hydroxides

The hydroxides considered in the study are amorphous Al hydroxide and Fe(II) and Fe(III) hydroxide.

Carbonates

Carbonates considered in the current study include calcite, dolomite, magnesite and siderite. The selection is based on carbonates commonly associated with basalt weathering and low temperature ($< 100^\circ$ C) thermal alteration, along with field observations from Marraat, a basalt hosted petroleum reservoir in Nuussuaq, West Greenland. Calcite is the only carbonate that is commonly found associated with basalt weathering and low temperature alteration in Iceland but three types of carbonates are found at

Marraat: magnesite-siderite solid solutions, dolomite with minor solid solutions of ankerite and near stoichiometric calcite (Rogers et al., 2006). Siderite and magnesite are allowed to precipitate as a solid solution, as observed in Marraat.

Zeolites

Zeolites are among the most common products of chemical interaction between groundwater and the Earth's crust during diagenesis and low-grade metamorphism (Neuhoff et al., 2000). Zeolites considered here include analcime, chabazite, heulandite, laumontite, mesolite, natrolite, stellerite and stilbite. Chabazite and heulandite form solid solutions between Ca- and Na-end-members. Stilbite and stellerite can also precipitate as a solid solution.

5. Thermodynamic relations

The key to performing geochemical solubility and speciation calculations stems from the laws of thermodynamics, stating that each system attempts to attain the state of lowest free energy. In most systems of geologic interest, the property to be minimized is the Gibbs free energy. The apparent standard molal Gibbs free energy ($\Delta G^0_{\mathrm{T,P}}$) of formation of minerals at temperature T and pressure P can be written as (e.g. Helgeson et al., 1978):

$$\begin{aligned}\Delta G^0_{T,P} =& \Delta G^0_f - S^0_{T_r,P_r}\,(T - T_r) + \int_{T_r}^{T} C^0_P \mathrm{dT} \\ & - T\int_{T_r}^{T} \frac{C^0_P}{T}\mathrm{dT} + \int_{P_r}^{P} V^0 \mathrm{dP}\end{aligned} \tag{1}$$

where ΔG^0_f denotes the standard Gibbs free energy of formation of the mineral in question from its elements in its stable phase at the reference pressure ($P_r = 1\,\mathrm{bar}$) and temperature ($T_r = 298.15\,\mathrm{K}$). $S^0_{T_r,P_r}$ is the standard molar entropy of minerals gases and aqueous species at T_r and P_r, C^0_P is the isobaric standard molar heat capacity at temperature T and V^0 is the standard molar isobaric volume.

The standard molar entropy ($S^0_{T,P}$) at a given temperature and pressure

is given by (Helgeson et al., 1978):

$$S^0_{T,P} = S^0_{T_r,P_r} + \int_{T_r}^{T} C^0_P \mathrm{d}\ln \mathrm{T} - T\int_{P_r}^{P}\left(\left(\frac{\partial V^0}{\partial P}\right)P\right)T\mathrm{dP} \tag{2}$$

Various relations describing the temperature variation of isobaric heat capacities of minerals have been developed. The simplest, widely used equation is most likely the Maier-Kelley power function (Kelley, 1960):

$$C^0_P = a + bT + cT^{-2} \tag{3}$$

where a, b and c are empirical fitting coefficients that are unique to the specified mineral from T_r to T. Equation 3 was e.g. widely used by Helgeson et al. (1978) in the creation of their mineral thermodynamic database. Other power functions describing isobaric heat capacities for minerals have e.g. been developed by Haas and Fisher (1976) and Berman and Brown (1985).

According to Helgeson et al. (1978), the most reliable method to obtain internally consistent thermodynamic data is through the regression of experimentally measured equilibrium pressure and temperature for a series of equilibria among minerals and/or a co-existing fluid phase. To perform these regressions, Helgeson et al. (1978) assumed that entropy and heat capacity was known through equations 2 and 3, respectively. By assuming mineral volumes to be independent of temperature and pressure, i.e.:

$$\int_{P_r}^{P} V^0\mathrm{dP} = V^0\left(P - P_r\right) \tag{4}$$

integration of equation 1 yields:

$$\begin{aligned} G^0_{T,P} - G^0_{T_r,P_r} = &- S^0_{T_r,P_r}(T - T_r) + a\left(T - T_r - T\ln\left(\frac{T}{T_r}\right)\right) \\ &- \left(\frac{(c + bT_r^2T)(T - T_r)^2}{2T_r^2 \cdot T}\right) + V^0(P - P_r) \end{aligned} \tag{5}$$

SUPCRT92 (Johnson et al., 1992) is a software package that applies the method of Helgeson et al. (1978) for calculating the standard molal thermodynamic properties of minerals, gases, aqueous species, and reactions from

1 to 5000 bar and 0 to 1000 °C. SUPCRT92 was used in the current study for calculating equilibrium solubility constants for minerals when measured values could not be directly incorporated to the dataset.

6. Methods

Sections 6.1 and 6.2 give detailed information on the methods used for computing equilibrium constants for the dissociation reactions of individual minerals and aqueous species given in table 3. Recently published thermodynamic data was compiled for most of the minerals considered in this study. Generally, $\log K$ values of minerals obtained directly from solubility measurements were incorporated to the dataset without modification. In a few cases equilibrium constants were taken from the EQ3/6 database but SUPCRT92 (Johnson et al., 1992) and the SLOP.98 modified SUPCRT database (Shock et al., 1997; Plyasunova et al., 2004) was used for computing $\log K$ values for other minerals. Attempts were made to maintain as much consistency as possible within the developed dataset as described in detail in following subsections.

In accord with the conventions adopted by Johnson et al. (1992), the standard state for pure minerals and liquids in this study is unit activity of the pure solid or liquid at any temperature and pressure. The standard state for aqueous species is unit activity of the species in a hypothetical one molal solution referenced to infinite dilution at any temperature and pressure. The gas standard state corresponds to unit fugacity at 1 bar and any temperature.

Aqueous species

Arnórsson and Andrésdóttir (1999) described the temperature dependence of the dissociation of Al-hydroxy complexes in aqueous solution by the following equations:

$$\begin{aligned}
\log K_1 &= -39.183 - 64.84/T - 29.515 \cdot 10^{-6} T^2 + 13.339 \log T \\
\log K_2 &= 43.638 - 3272.37/T - 9.745 \cdot 10^{-6} T^2 - 16.354 \log T \\
\log K_3 &= 16.962 - 2096.03/T - 10.262 \cdot 10^{-6} T^2 - 6.818 \log T \\
\log K_4 &= 97.711 - 5237.63/T + 9.840 \cdot 10^{-6} T^2 - 35.498 \log T
\end{aligned} \tag{6}$$

where K_1 to K_4 represent equilibrium constants for stepwise dissociation of $Al(OH)_n^{3-n}$. The equations are valid in the range 0-350° C at 1 bar below

100° C and at vapor saturation pressures at higher temperature and were used for computing $\log K$ values for the reactions involving Al-hydroxy complexes in table 3.

6.1. Primary basaltic minerals and glasses

Basaltic glass composition was taken from Oelkers and Gíslason (2001). TiO_2 and P_2O_5, which make up 1.564 and 0.195 weight % of the total glass composition, respectively, were ignored. This was done because titanium and phosphorus are not included in the system being modeled. Ferric iron (Fe_2O_3) was stoichiometrically replaced with ferrous iron (FeO) as using both oxidation states as primary species can cause problems in numerical simulations. Equilibrium and supply of $O_{2\,(aq)}$ governs oxidation of Fe(II) dissolved from primary minerals to Fe(III) in the simulations, as shown in table 3. Resulting chemical composition of the Stapafell glass normalized to one Si atom is: $Si\,Al_{0.36}\,Fe(II)_{0.19}\,Mg_{0.28}\,Ca_{0.26}\,Na_{0.08}\,K_{0.008}\,O_{3.31}$.

Calculations of log(K) values for dissolution of basaltic glass are based on a theoretical approach originally proposed by Paul (1977) that considers the glass to be an oxide mixture. Thus, the solubility of the material can be estimated from the ideal solid solution relation:

$$\log(K)_{\text{glass}} = \sum_i \log(K_i) + \sum_i x_i \log x_i \tag{7}$$

where x_i and K_i are the mole fractions and solubility products of the glass-constituting oxides. Table 4 shows the oxide dissolution reactions and $\log K_i$ values used for calculating equilibrium constants for the basaltic glass at various temperature. This method of estimating solubility products of borosilicate and aluminosilicate glasses has already been successfully applied by e.g. Bourcier et al. (1992), Advocat et al. (1998) and Leturcq et al. (1999). Techer et al. (2001) also obtained a good result using the same approach to model the dissolution of synthetic basaltic glass at 90° C.

Crystalline basalt – Olivine, plagioclase and pyroxene

Stefánsson (2001) derived the solubility constants of primary minerals of basalt in pure water in the temperature range of 0-350° C at saturated water vapor pressure. The thermodynamic data used by Stefansson is consistent with the data used in this study. As Stefánsson also uses the same primary species, reported $\log K$ values for olivine, plagioclase and pyroxene could be incorporated to the current dataset without further modification.

6.2. Secondary minerals

Silicates

Gunnarsson and Arnórsson (2000) determined the solubility of amorphous silica and quartz in the temperature range of 0° to 350° C at 1 bar below 100° C and at P_{sat} at higher temperature. They retrieved the following temperature equations describing amorphous silica and quartz solubility:

$$\log K_{am.silica} = -8.476 - 485.24T^{-1} - 2.268 \cdot 10^{-6}T^2 + 3.068 \log T \quad (8)$$

$$\log K_{quartz} = -34.188 + 197.47T^{-1} - 5.851 \cdot 10^{-6}T^2 + 12.245 \log T \quad (9)$$

where T is in K. Equations 8 and 9 were used for calculating equilibrium constants for amorphous silica and quartz.

Gunnarsson et al. (2005) carried out magnesium silicate precipitation experiments in alkaline solutions in the temperature range of 39° to 150° C and determined e.g. the solubility of poorly crystalline antigorite. They retrieved the following temperature equation, describing antigorite solubility:

$$\log K_{antigorite} = 9303 \cdot T^{-1} + 3.283 \quad (10)$$

where T is in K. Equation 10 is valid in the temperature range of 0° to 200° C and was used for calculating equilibrium constants for antigorite dissolution.

$\log K$ values for montmorillonite were taken from the EQ3/6 database (Wolery, 1992). Equilibrium constants for other silicates were computed with SUPCRT92 using the molal properties in table 6. Thermodynamic data for celadonite, Fe-celadonite and kaolinite was taken from Holland and Powell (1998) but allophane and imogolite data from Stefánsson and Gíslason (2001). Heat capacity polynomials for allophane and imogolite were not found in the literature so computed $\log K$ values cannot be extrapolated to temperature higher than 25°C.

Gíslason et al. (1997) determined thermodynamic properties for end-member moganite from 25° to 200° C. Standard state enthalpy, entropy and Gibbs free energy can be found in table 6. The standard state molal properties of moganite and the heat capacity function for quartz (also shown in table 6) were used to calculate equilibrium constants for moganite at different temperature. Calculations were performed using SUPCRT92 and the slop98 database.

The thermodynamic properties of aqueous silica and silica polymorphs used in the current study are consistent with data published by Gunnarsson and Arnórsson (2000), Rimstidt (1997) and Apps (1970), which differ from the data of Helgeson et al. (1978) that is incorporated to the SUPCRT database. For consistency, $SiO_{2\,(aq)}$ was replaced with quartz in the dissolution reactions given in table 3 for moganite, celadonite, chlorite, kaolinite, allophane and imogolite and SUPCRT92 used along with the standard molal properties given in table 6 for computing corresponding $\log K$ values. Resulting values were then converted to the reactions, shown in table 3, by adding both the reaction and $\log K$ values for the dissolution of quartz to $SiO_{2\,(aq)}$.

Hydroxides

Equilibrium constants for Fe(II) and Fe(III) hydroxide dissolution were taken from the EQ3/6 database (Wolery, 1992). Standard state enthalpy, entropy and Gibbs free energy for amorphous Al hydroxide were obtained from Stefánsson and Gíslason (2001). Heat capacity polynomials for Al hydroxide were not found in the literature. Equilibrium constants for Al hydroxide can, therefore, not be extrapolated to temperature higher than 25°C.

Carbonates

Equilibrium constants for dissolution of calcite, dolomite and magnesite were calculated with SUPCRT92 using thermodynamic data from Holland and Powell (1998).

Bénézeth et al. (2009) investigated the solubility of siderite from 25-250° C and obtained the following function that describes solubility as a function of temperature:

$$\log K_{siderite} = 175.568 + 0.0319 \cdot (T) - 6738.483 \cdot (T)^{-1} - 67.898 \cdot \log(T) \quad (11)$$

where T is in K. Based on equation 11, along with its first and second derivatives with respect to T, Bénézeth et al. (2009) were able to derive values for the Gibbs energy of formation, enthalpy of formation, entropy and siderite heat capacity. Corresponding values can be found in table 6. Equation 11 was used directly to generate $\log K$ values for the dissolution of siderite. As Bénézeth et al. (2009) expressed the dissolution reaction in terms of CO_3^{2-} instead of HCO_3^-, resulting $\log K$ values were transformed to the dissolution reaction given in table 3 by adding equilibrium reaction and corresponding $\log K$ values between CO_3^{2-} and HCO_3^-.

Zeolites

Fridriksson et al. (2001) provide reference thermodynamic data that can be used to compute $\log K$ values for stellerite and stilbite. The authors derived their data from experimental studies and field measurements of the solubility of stellerite-stilbite solid solutions in geothermal waters. Their reference data for stellerite was calculated using Gibbs free energies from Helgeson et al. (1978) for reactants and products, which differ from the reference data used in the current dataset. For consistency with the study of Fridriksson et al., SUPCRT92 was used to compute $\log K$ values for the following reactions, using the same reference data as these authors for all reactants and products:

$$\text{stellerite} + \text{Na}^+ = \text{albite} + \text{quartz} + 2\,\text{Ca}^{2+} + 14\,\text{H}_2\text{O} \tag{12}$$

$$\text{stilbite} + 4\,\text{chalcedony} = \text{stellerite} + \text{albite} + 2\,\text{H}_2\text{O} \tag{13}$$

The $\log K$ values obtained with SUPCRT92 were then converted for the reactions, shown in table 3, expressing the full dissolution of stellerite and stilbite. In the case of stellerite, this was done by adding the reactions and $\log K$ values for albite and quartz dissolution used in the present study to equation 12. For stilbite, on the other hand, reactions and $\log K$ values for chalcedony, albite and stellerite were subtracted or added to equation 13. $\log K$ values used for quartz are those given in table 7 but values for albite and chalcedony are from the Yucca Mountain thermodynamic database (Spycher et al., 2007), which is consistent with the current dataset. Albite data is based on the work of Arnórsson and Stefánsson (1999).

Thermodynamic data for other zeolites than stellerite and stilbite was taken from Neuhoff (2000). Similar approach, as described above for stellerite and stilbite, was used for computing $\log K$ values for analcime, laumontite and Ca-heulandite as Neuhoff used different reference data for obtaining thermodynamic properties for these minerals. For consistency, SUPCRT92 was thus used to compute $\log K$ values for the following reactions, using the same reference data as Neuhoff for all reactants and products:

$$\text{analcime} + 0.84\,\text{quartz} = 0.96\,\text{albite} + \text{H}_2\text{O} \tag{14}$$

$$\begin{aligned} \text{laumontite} &= \text{leonhardite} + \mathrm{H_2O} \\ &= \text{wairakite} + 2.5\,\mathrm{H_2O} \\ &= \text{anorthite} + 2\,\text{quartz} + 4.5\,\mathrm{H_2O} \end{aligned} \tag{15}$$

$$\begin{aligned} \text{Ca} - \text{heulandite} &= \text{leonhardite} + 3\,\text{quartz} + 2.5\,\mathrm{H_2O} \\ &= \text{anorthite} + 5\,\text{quartz} + 6\,\mathrm{H_2O} \end{aligned} \tag{16}$$

The $\log K$ values obtained with SUPCRT92 for reactions 14 - 16 were then converted to the reactions shown in table 3 that express the full dissolution of analcime, laumontite and Ca-heulandite by adding reactions and $\log K$ values for the corresponding minerals. $\log K$ values for anorthite were taken from the Yucca Mountain thermodynamic database (Spycher et al., 2007) and are based on the work of Arnórsson and Stefánsson (1999). Table 5 gives the dissolution reactions and equilibrium constants for albite, anorthite and chalcedony used for converting SUPCRT dissolution reactions and computed $\log K$ values for analcime, laumontite, Ca-heulandite, stellerite and stilbite to the reactions shown in table 3.

Neuhoff used a method based on summation of the contributions of compositional units to thermodynamic properties for the remaining zeolites considered in this study, i.e. Ca,Na-chabazite, Na-heulandite, mesolite and natrolite (see Neuhoff et al., 1999, for further detail). For consistency, $\mathrm{SiO_{2\,(aq)}}$ was replaced with quartz in the dissolution reactions of these zeolites when computing $\log K$ values with SUPCRT92, and the results corrected afterwards by adding dissolution of quartz to $\mathrm{SiO_{2\,(aq)}}$.

7. Results

Tables 6 and 7 show, respectively, standard molal thermodynamic properties for the minerals considered in this study along with their corresponding equilibrium constants at eight different temperatures (0, 25, 60, 100, 150, 200, 250 and 300 °C). The equilibrium constants presented in table 7 can be incorporated into other thermodynamic databases without further modification, provided that the databases used are set up with respect to the basis set of aqueous species as used in this study.

8. Database evaluation

In order to verify that the dataset presented in tables 2-7 delivers reliable results, simulations of CO_2-water-basalt interaction were carried out at low and elevated CO_2 conditions and compared to observed alteration in Iceland and Greenland. First, basalt alteration in the Hellisheidi CO_2 injection site in SW-Iceland was simulated. Second, elevated CO_2-water-basalt interaction simulations were carried out in order to see if alteration assemblages observed in the basalt hosted petroleum reservoir in Marraat, W-Greenland could be regenerated.

8.1. Basalt alteration in Hellisheidi

A pilot scale CO_2 injection is ongoing in Iceland with the objective of assessing the feasibility of *in situ* CO_2 mineral sequestration in basaltic rocks (see e.g. Aradóttir et al., 2011; Gíslason et al., 2010; Matter et al., 2008; Oelkers et al., 2008, for further detail). Extensive research has been conducted in order to characterize the pilot injection site at Hellisheidi with respect to stratigraphy, hydrology as well as other physical and chemical properties (e.g. Aradóttir et al., 2011; Níelsson, 2011; Helgadóttir et al., 2010; Gíslason et al., 2010; Alfredsson et al., 2008; Rezvani Khalilabad et al., 2008). Near horizontal sequences of basalt lavas and basaltic glass formations govern the bedrock. Common alteration minerals in the low-temperature region ($T < 100\,^{\circ}C$) include clay minerals, calcite and zeolites. At higher temperature, pyrite, quartz, epidote and prehnite become abundant. The horizontal zeolite zones so commonly found in Iceland and initially described by Walker (1960) are clearly detectable at Hellisheidi. Figure 1 gives a simplified view of the alteration zones along with their approximate depth and temperature range.

8.2. Simulations

A series of batch simulations involving low pCO_2 water-basalt interactions were carried out in the temperature and pressure range corresponding to conditions between 200 and 1000 m depth below surface in Hellisheidi (i.e. between 5 and 120 ° and 10-110 bars, respectively). Initial water composition was that of the shallow well HK-21 in Hellisheidi. The water is of non-geothermal origin and only a few years old (Árnason et al., 1969). Basaltic glass, plagioclase, olivine and pyroxene were used as primary minerals in the batch simulations. Initial water and bedrock compositions are given in table

8. All secondary minerals in the dataset presented in tables 2, 3, 6 and 7 were compiled as potential alteration minerals in the simulations, which were run for up to 10,000 years using the TOUGHREACT simulator. Equilibrium and supply of $O_{2\,(aq)}$ governs oxidation of Fe(II) dissolved from primary minerals to Fe(III) in the simulations, as shown in table 3.

In order to see what effect elevated CO_2 conditions have on basalt alteration, simulations were also carried out with pCO_2 as high as 40 bars and results compared to the basalt alteration in Marraat, W-Greenland, reported by Rogers et al. (2006) and described in section 2. Primary rock composition was assumed to be the same as in Hellisheidi as corresponding data from Greenland was lacking. Initial water composition was also assumed to be the same as that given in table 8, except that CO_2 (DIC) concentrations equaled Henry's law saturation at 10, 20, 30 and 40 bar CO_2 pressure. Simulations carried out did thus only involve single phase conditions.

8.3. Results

Figure 2 shows comparison of observed and simulated alteration mineralogy in Hellisheidi. Overall there is good agreement between simulated alteration and alteration observed in the field. Results for clay minerals, simple oxides and hydroxides, calcite and $SiO_{2\,(s)}$ are in good agreement with field observations and same goes for chabazite, mesolite, laumontite, heulandite and stilbite-stellerite. Analcime is observed Hellisheidi between 400 and 800 m depth but does not form in simulations as dissolved Na appears to preferably go into stilbite-stellerite, most likely due to more flexibility in the solid solution compared to the fixed analcime composition. Upon removal of stellerite-stilbite from potential alteration minerals, analcime formed instead.

Elevating CO_2 concentrations of initial water in the batch series simulations completely changed the picture shown in figure 2. At elevated CO_2 conditions, substantial formation of quartz, moganite and/or amorphous SiO_2 inhibits the uptake of Ca, Mg and Fe into zeolites and clay minerals. As a result, the clays and zeolites shown in figure 2 are replaced by magnesite, siderite, dolomite and also calcite at temperature above 50° C. Al is removed into hydroxides and simple aluminum silicates. These results are in good agreement with reports from Marraat in Greenland, which are summarized in table 1. In Marraat, migration of petroleum into altered basalt led to the pseudomorphic replacement of zeolite and clay mineral assemblages with carbonates and quartz. Magnesite-siderite solid solutions and dolomite predominantly formed at Marraat but at later stages, also calcite. Simulated

basalt alteration under elevated CO_2 conditions are also in good agreement with batch experiments carried out by Gysi (2011) aimed at studying basaltic glass alteration under elevated CO_2 pressures (7-24 bar) and hydrothermal conditions (75-250° C). Between 75-150° C, alteration minerals mainly consisted of Ca-Mg-Fe carbonate solid solutions and SiO_2 minerals. The mineral assemblage observed in the experiments thus compares nicely with the assemblage predicted by the batch simulations. Figure 3 compares the simulations carried out to natural observations in Greenland and experiments carried out by Gysi (2011). Larger uncertainties are associated with natural pressure and temperature conditions in figure 3 than the data shown in figure 2. Figure 3 nevertheless shows good conformity between the overall alteration mineral assemblages observed in Greenland, laboratory experiments and simulations carried out in this study.

9. Discussion

The batch simulations described above were carried out in order to evaluate how well the developed dataset was able to reproduce alterations close to what is observed in nature. Match between modeled and natural alterations was good for both low and elevated CO_2 conditions, which implies that the dataset should be well suited for geochemical simulations of CO_2 mineral sequestration in basalts as well as other CO_2-water-basalt interaction processes. Data from natural analogs of basalt alteration under low CO_2 conditions was abundant, e.g. due to extensive studies of well drill cuttings in Iceland, whereas data from natural analogs of basalt alteration under elevated conditions was not as comprehensive. Consequently, it was not possible to compare modeled and observed basalt alteration at elevated CO_2 conditions in as much detail as at low CO_2 conditions. Looking forward, it is of great importance to acquire more detailed laboratory and field data on water-basalt interaction under elevated CO_2 conditions as that would allow for a more detailed fine-tuning of thermodynamic databases.

The thermodynamic dataset presented in this contribution provides data at 1 bar pressure up to 100° C, and along the boiling curve of water at higher temperature. The simulations carried out, however, involve pressure above 1 bar at temperature below 100° C, which introduces some uncertainties into simulation results. Millero (1982) studied the effect of pressure on the solubility of minerals in water and seawater and showed that the between 10-100 bars, pressure changes only had a very slight effect on silicate solubility and

only a small effect on calcite solubility. At the maximum pressure of 100 bars, the increase in calcite solubility in freshwater and seawater was estimated to be around 0.2 to 0.25 at 25° C (see figures 5 and 6 in Millero, 1982). This translates into a difference of less than 0.11 in the logK solubility of calcite, which is likely to be within the uncertainty in the calcite solubility, given that there are numerous substituting cations in calcite (such as Mg and Sr) that reduce the solubility of calcite but are not taken into account in the thermodynamic description of calcite. According to the results of Millero (1982), uncertainties associated with applying the developed dataset in simulations involving pressure above 1 bar at temperature below 100° C, should therefore be small.

This study considered plagioclase, pyroxene, olivine and basaltic glass as primary phases in basalt. Fe-Ti oxides (titanomagnetite and ilmenite) and apatite were thus omitted. This was done in view of the necessity of constraining and simplifying the simulated system. Multidimensional field scale reactive transport simulations of CO_2 mineral sequestration in basalts are extremely computationally demanding and it is, therefore, important to limit the number of species and minerals included in the models. Fe-Ti oxides and apatite have been reported to be of low abundance (see e.g. Gudbrandsson et al., 2011) and low reactivity (Arnórsson et al., 2002) in Icelandic basalts. Arnórsson et al. (2002) studied primary mineral saturation in basalt hosted groundwaters in N-Iceland and showed that the waters were under-saturated with respect to plagioclase and olivine and close to saturation with augite, while being over-saturated with titanomagnetite at temperature below 70°C and highly over-saturated with respect to apatite. In view of this, it was found satisfactory to only consider plagioclase, pyroxene, olivine and basaltic glass as primary phases of basalts in Iceland. Stefánsson (2001) has estimated the mineral solubility of various apatite and Fe-Ti oxide end-members and the resulting values can be included in the current dataset without modification. Adding these minerals to future simulations would therefore not require much additional work, only faster geochemical simulators for the simulations to be practical.

Ferric iron can account for a significant amount of iron in basaltic glass (e.g. Oelkers and Gíslason, 2001). Using both iron oxidation states as primary species in reactive transport simulations is a challenging task due to limited knowledge on kinetics between the two oxidation states. Ferric iron was, therefore, stoichiometrically replaced with ferrous iron in the basaltic glass considered in this study. As Fe(II) is released during simulated dissolu-

tion, equilibrium and supply of $O_{2\,(aq)}$ governs oxidation of Fe(II) to Fe(III), as shown in table 3. Experimental data on the kinetics of redox reactions between Fe(II) and Fe(III) are needed in order to improve numerical models with respect to iron.

In addition to the 10 zeolites found in the dataset, gismondine, levyne, phillipsite, scolecite, mordenite and thomsonite are also common secondary minerals in basalt. These zeolites are, however, not considered here for the following reasons. Epistilbite, gismondine and levyne were omitted as thermodynamic data for these zeolites was not found in the literature. The published thermodynamic data found for phillipsite (from the EQ3/6 database, Wolery (1992)), scolecite, mordenite and thomsonite (from Neuhoff et al. (1999)) gave unrealistic results in simulations of CO_2-water-basalt interaction. When these particular zeolites were included in geochemical simulations they precipitated in such immense quantities that all other alteration reactions became derailed and simulation results were unrealistic. This could have been the result of uncertainties or errors in the published thermodynamic data or due to the non-ideality (Fridriksson et al., 2003a,b; Neuhoff and Bird, 2001; Neuhoff et al., 2003) and cation exchange mechanisms observed in zeolites (Fridriksson et al., 2004), both of which current reaction path and reactive transport models are not capable of simulating. Consequently, phillipsite, scolecite, mordenite and thomsonite had to be omitted from this study. It would be of great importance for numerical modeling of CO_2 mineral sequestration in basalts if the solubility constants of these zeolites could be re-evaluated in laboratory experiments in the near future.

Simulations described in this paper were aimed at evaluating how well the developed dataset was able to capture basalt observations in natural analogs of water-basalt interaction under low and elevated CO_2 conditions. Simulations, thus, mainly treated mineral dissolution and precipitation as a purely equilibrium problem. Equivalent simulations were carried out using reaction kinetics to estimate how sensitive modeled alteration mineralogy was to kinetic control of reaction. Mineral dissolution in the sensitivity simulations was described through a pH dependent rate law using predominantly rate law equations from Palandri and Kharaka (2004). Alteration mineral assemblage was not affected by incorporating reaction kinetics into batch simulations. However, relative abundance of individual alteration minerals was affected. Compilation of the dataset discussed in this paper is a part of modeling activities carried out with the objective of developing multidimensional field scale reactive transport models of CO_2 mineral sequestration

in Icelandic basalts, as has already been mentioned. Developed models all consider reactions kinetics as is described in detail in Aradóttir (2011).

10. Conclusions

Compilation and evaluation of a thermodynamic database is a tedious and time-consuming process. It is nonetheless a necessary step of all modeling work, as widely used databases that are included in geochemical software packages not always contain minerals or thermodynamic data suitable for geochemical simulations of a particular problem or process, as e.g. discovered in this study. We have developed a thermodynamic dataset describing 36 mineral reactions of interest for CO_2-water-basalt interaction. Mineral selection for the dataset is based on extensive review of natural analogs of water-basalt interaction at low and elevated CO_2 conditions. In order to verify that the dataset delivers reliable results, simulations of CO_2-water-basalt interaction were carried out at low and elevated CO_2 conditions and results compared to observed alteration in Iceland and Greenland. Overall good agreement is observed between simulated and natural alteration both at low and elevated CO_2 conditions, suggesting that the dataset is well suited for simulating CO_2 mineral sequestration in basalts as well as other processes applicable to CO_2-water-basalt interaction.

The presented dataset, like all other databases, should be thought of as being a work in progress rather than a completed task. Looking forward it is of great importance to acquire more detailed laboratory and field data on water-basalt interaction under elevated CO_2 conditions as that would allow for further fine-tuning of the database. It would also be of great importance to measure and/or re-evaluate the solubility constants of the zeolites that had to be omitted in the current version of the database, particularly for thomsonite and scolecite.

Acknowledgments

We are grateful to Prof. Dennis K. Bird at Stanford University for his constructive input to this work. We thank Bergur Sigfússon, Einar Gunnlaugsson, Gretar Ívarsson and Ingvi Gunnarsson at Reykjavík Energy for helpful discussions and support. We also thank Nic Spycher, John Apps and Karsten Pruess at Lawrence Berkeley National Laboratory, Andri Stefánsson, Helgi

A. Alfredsson, Sigurdur R. Gíslason and Snorri Gudbrandsson at the Institute of Earth Sciences at the University of Iceland and Gunnlaugur Einarsson at Iceland GeoSurvey.

This work was funded by Reykjavík Energy, Geothermal Research Group GEORG (09-01-003 and 09-02-001) and the University fund of Eimskipafélag Íslands.

References

Advocat, T., Chouchan, J. L., Crovisier, J. L., Guy, G., Daux, V., Jégou, C., Gin, S., Vernaz, E., 1998. Borosilicate nuclear waste glass alteration kinetics: chemical inhibition and affinity control. In: Mater. Res. Soc. Vol. 506. pp. 63–70.

Alfredsson, H., Hardarson, B., Franzson, H., Gślason, S., 2008. CO_2 sequestration in basaltic rock at the Hellisheidi site in SW Iceland: Stratigrapy and chemical position of the rocks at the injection site. Mineral. Mag. 72, 1–5.

Apps, J. A., 1970. The Stability Field of Analcime. Ph.D. thesis, Harvard University, Cambridge, Massachusetts.

Aradóttir, E. S. P., 2011. Reactive transport models of CO_2-water-basalt interaction and applications to CO_2 mineral sequestration. Ph.D. thesis, Faculty of Physical Sciences, University of Iceland.

Aradóttir, E. S. P., Sigurdardóttir, H., Sigfússon, B., Gunnlaugsson, E., 2011. CarbFix – a CCS pilot project imitating and accelerating natural CO_2 sequestration. Greenhouse Gases: Science and Technology 1, 105–118.

Arnalds, O., 1990. Characterization and erosion of andisols in Iceland. Ph.D. thesis, Texas A&M University.

Arnalds, O., Hallmark, C., Wilding, L., 1995. Andisols from four different regions of Iceland. Soc. Amer. J. 59, 161–169.

Árnason, B., Theódorsson, P., Björnsson, S., Saemundsson, K., 1969. Hengill, a high temperature thermal area in Iceland. Bulletin Volcanologique 33, 245–259.

Arnórsson, S., 1999. The relative abundance of Al-species in natural waters in Iceland. In: Geochemistry of the Earth's Surface.

Arnórsson, S., Andrésdóttir, A., 1999. The dissociation constants of Al-hydroxy complexes at 0-350° C and P_{sat}. In: Geochemistry of the Earth's Surface.

Arnórsson, S., Gunnarsson, I., Stefánsson, A., Andrésdóttir, A., Sveinbj̈ornsdottir, A., 2002. Major element chemistry of surface- and groundwaters in basaltic terrain, N-Iceland. I. Primary mineral saturation. Geochim. Cosmochim. Acta 66, 4015–4046.

Arnórsson, S., Sigurdsson, S., Svavarsson, H., 1982. The chemistry of geothermal waters in Iceland. I. Calculation of aqueous speciation from 0 to 370°C. Geochim. Cosmochim. Acta 46, 1513–1532.

Arnórsson, S., Stefánsson, A., 1999. Assessment of Feldspar Solubility Constants in Water in the Range 0° to 350°C at Vapor Saturation Pressure. Am. J. Sci. 299, 173–209.

Bénézeth, P., Dandurand, J., Harrichoury, J., 2009. Solubility product of siderite ($FeCO_3$) as a function of temperature (25 - 250 °C). Chem. Geol. 265, 3–12.

Berman, R. G., Brown, T. H., 1985. Heat Capacities of minerals in the system Na_2O-K_2O-CaO-MgO-FeO-Fe_2O_3-Al_2O_3-SiO_2-TiO_2-H_2O-CO_2. Representation, estimation and high temperature extrapolation. Contrib. Mineral. Petrol. 89, 168–183.

Bjarnason, J. O., 1994. The speciation program WATCH, version 2.1. Icelandic Natl. Energy Aut. Rep., 7 pp.

Blanc, P., A., L., Piantone, P., 2009. Thermoddem, a thermodynamic database for modelling the alteration of waste minerals.
URL `http://thermoddem.brgm.fr/`

Bourcier, W., Weed, H., Nguyen, S., Nielson, J., Morgan, L., Newton, L., Knauss, K., 1992. Solution compositional effects on dissolution kinetics of borosilicate glass. In: Kharaka, Y., Maest, A. (Eds.), WRI-7 Symposium proceedings. Balkema, Rotterdam. pp. 81–84.

Crovisier, J., Honnerez, J., Fritz, R., Petit, J., 1992. Dissolution of subglacial volcanic glasses from Iceland. Laboratory study and modeling. Applied Geochem. Suppl. 1, 55–81.

Delaney, J. M., Wolery, T. J., 1989. The LLNL thermochemical database. Report UCRL-21658.

Engi, M., 1992. Thermodynamic data for minerals: a critical assessment. In: Price, G. D., Ross, N. L. (Eds.), The Stability of Minerals. Kluwer Academic Publishers, Dordrecht, pp. 267–329.

EU, April 2009. Directive 2009/31/ec on the geological storage of carbon dioxide. Online.
URL http://eur-lex.europa.eu/LexUriServ/LexUriServ.do?uri=OJ:L:2009:140:0114:0135:EN:PDF

Flörke, O., Jones, J., Schmincke, H., 1976. A new microcrystalline silica from Gran Canaria. Zeit. Krist. 143, 156–165.

Franzson, H., Gunnlaugsson, E., Árnason, K., Saemundsson, K., Steingrḿsson, B., Hardarson, B. S., 2010. The Hengill Geothermal System, Conceptual Model and Thermal Evolution. In: Proceedings, World Geothermal Congress, Bali, Indonesia, 25-29 April.

Fridriksson, T., Bish, D. L., Bird, D. K., 2003a. Hydrogen-bonded water in laumontite I: X-ray powder diffraction study of water site occupancy and structural changes in laumontite during room-temperature isothermal hydration/dehydration. Am. Mineral. 88, 277–287.

Fridriksson, T., Carey, J. W., Bish, D. L., Neuhoff, P. S., Bird, D. K., 2003b. Hydrogen-bonded water in laumontite II: Experimental determination of site-specific thermodynamic properties of hydration of the W1 and W5 sites. Am. Mineral. 88, 1060–1072.

Fridriksson, T., Neuhoff, P., Arnórsson, S., Bird, D., 2001. Geological constraints on the thermodynamic properties of the stilbite-stellerite solid solution in low-grade metabasalts. Geochim. Cosmochim. Acta 65, 3993–4008.

Fridriksson, T., Neuhoff, P. S., Viani, B. E., Bird, D. K., 2004. Experimental determination of thermodynamic properties of ion-exchange in heulandite:

Binary ion exchange experiments at 55 and 85 ∘c involving Ca^{2+}, Sr^{2+}, Na^{+} and K^{+}. Am. J. Sci. 304, 287–332.

Gíslason, S., Heaney, P., Oelkers, E., Schott, J., 1997. Kinetic and thermodynamic properties of moganite, a novel silica polymorph. Geochim. Cosmochim. Acta 61, 1193–1204.

Gíslason, S., Oelkers, E., 2003. Mechanisms, rates and consequences of basaltic glass dissolution: II. An experimental study of the dissolution rates of basaltic glass as a funciton of temperature. Geochim. Cosmochim. Acta 67, 3817–3832.

Gíslason, S. R., Wolff-Boenisch, D., Stefánsson, A., Oelkers, E. H., Gunnlaugsson, E., Sigurdardóttir, H., Sigfússon, B., Broecker, W. S., Matter, J. M., Stute, M., Axelsson, G., Fridriksson, T., 2010. Mineral sequestration of carbon dioxide in basalt: A pre-injection overview of the CarbFix project. Int. J. of Greenhouse Gas Control 4, 537–545.

Gudbrandsson, S., Wolff-Boenisch, D., Gíslason, S., Oelkers, E., 2011. An experimental study of crystalline basalt dissolution from $2 \leq$ pH ≤ 11 and temperatures from 5 to 75 °C. Geochim. Cosmochim. Acta 75, 5496–5509.

Gunnarsson, I., Arnórsson, S., 2000. Amorphous silica solubility and the thermodynamic properties of H_4SiO_4 in the range of 0 to 350°C at P_{sat}. Geochim. Cosmochim. Acta 64, 2295–2307.

Gunnarsson, I., Arnórsson, S., Jakobsson, S., 2005. Precipitation of poorly crystalline antigorite under hydrothermal conditions. Geochim. Cosmochim. Acta 69, 2813–2828.

Gysi, A., 2011. Co_2-water-basalt Interaction: Reaction Path Experiments and Numerical Modeling. Ph.D. thesis, Faculty of Earth Sciences, University of Iceland.

Haas, J. L. J., Fisher, J. R., 1976. Simultaneous evaluation and correlation of thermodynamic data. Am. J. Sci. 276, 525–545.

Helgadóttir, H. M., Snaebjörnsdottir, S. O., Níelsson, S., Gunnarsdóttir, S. H., Matthíasdóttir, T., Hardarson, B. S., Einarsson, G. M., Franzson, H., 2010. Geology and Hydrothermal Alteration in the Reservoir of the

Hellisheidi High Temperature System, SW-Iceland. In: Proceedings, World Geothermal Congress, Bali, Indonesia, 25-29 April.

Helgeson, H. C., Delaney, J. M., Nesbitt, H. W., Bird, D. K., 1978. Summary and critique of the thermodynamic properties of rock forming minerals. Am. J. Sci. 278A, 1–229.

Holland, T., Powell, R., 1998. An internally consistent thermodynamic data set for phases of petrological interest. J. Metam. Geol. 16, 309–343.

Johnson, J., Oelkers, E., Helgeson, H., 1992. SUPCRT92: a software package for calculating the standard molal thermodynamic properties of minerals, gases, aqueous species and reactions from 1 to 5000 bars and 0 to 1000 degrees C. Comput. Geosci. 18, 899–947.

Kelley, K. K., 1960. Contributions to the data on theoretical metallurgy. XIII. High tempterature heat content, heat capacity and entropy data for elements and inorganic compounds. US Bur. Mines Bull. 548, 232.

Kristmannsdóttir, H., Tómasson, I., 1978. Zeolite zones in geothermal areas in Iceland in Natural zeolites. Pergamon Press.

Leturcq, G., Berger, G., Advocat, T., Vernaz, E., 1999. Initial and long-term dissolution rates of aluminosilicate glasses enriched in Ti, Zr and Nd. Chemical Geology 160, 39–62.

Matter, J., Broecker, W., Stute, M., Gíslason, S., Oelkers, E., Stefánsson, A., Wolff-Boenisch, D., Gunnlaugsson, E., Axelsson, G., Björnsson, G., 2008. Permanent carbon dioxide storage into basalt: the CarbFix pilot project, Iceland. In: Proceedings of the 9th International Conference on Greenhouse Gas Control Technologies, 16-20 Nov, Washington DC, USA.

Millero, F., 1982. The effect of pressure on the solubility of minerals in water and seawater. Geochim. Cosmochim. Acta 46, 11–22.

Neuhoff, P., 2000. Thermodynamic properties of parageneses of rock-forming zeolites. Ph.D. thesis, Stanford University, Stanford, Calif.

Neuhoff, P., Fridriksson, T., Arnorsson, S., Bird, D., 1999. Porosity changes and mineral paragenesis during low-grade metamorphism at Teigarhorn, eastern Iceland. Amer. J. Sci. 299, 467–501.

Neuhoff, P. S., Bird, D. K., 2001. Partial dehydration of laumontite: thermodynamic constraints and petrogenetic implications. Mineral. Mag. 65, 1–12.

Neuhoff, P. S., Fridriksson, T., Bird, D. K., 2000. Zeolite Parageneses in the North Atlantic igneous Province: Implications for Geotectonics and Groundwater Quality of Basaltic Crust. International Geology Review 42, 15–44.

Neuhoff, P. S., Stebbins, J. F., Bird, D. K., 2003. Si-Al disorder and solid solution in analcime, chabazite and wairakite. Am. Mineral. 88, 410–423.

Níelsson, S., 2011. Geology and alteration in the Hverahlíd geothermal systemt in Hellisheidi. Master's thesis, Faculty of Earth Sciences, University of Iceland, in Icelandic.

Oelkers, E., Gíslason, S., 2001. The mechamism, rates and consequences of basaltic glass dissolution: I. An experimental study of the dissolution rates of basaltic glass as a function of aqueous Al, Si and oxalic acid concentrations at 25°C and pH = 3 and 11. Geochim. Cosmochim. Acta 65, 3671–3681.

Oelkers, E., Gíslason, S., Matter, J., 2008. Mineral Carbonation of CO_2. Elements 4, 331–335.

Oelkers, E. H., Bénézeth, P., Pokrovski, G. S., 2009. Thermodynamic Databases for Water-Rock Intereaction. Rev. Mineral. Geochem. 70, 1–56.

Palandri, J., Kharaka, Y., 2004. A compilation of rate parameters of water-mineral interaction kinetics for application to geochemical modeling. Report 2004-1068.

Parkhurst, D., Thorstenson, D., Plummer, L., 1980. PHREEQC:a computer program for geochemical calculations. US Geol. Surv., Water Resour. Investig. (80-96).

Parkhurst, D. L., Appelo, C. A. J., 1999. User's Guide to PHREEQC (Version 2) – A computer program for speciation, batch-reaction, one-dimensional reactive transport and inverse geochemical calculations. US Geol. Suv. Water Res. Inv. Report 99-4259.

Paul, A., 1977. Chemical durability of glasses, a thermodynamic approach. Journal of Material Science 12, 2246–2268.

Plyasunova, N., Plyasunov, A., Shock, E., 2004. Database of thermodynamic properties for aqueous organic compounds. International Journal of Thermophysics 25, 351–360.

Reed, M., Palandri, J., 2006a. SOLTHERM.H06, a data base of equilibrium constants for minerals and aqueous species. Available from the authors.

Reed, M., Palandri, J., 2006b. Sulfide Mineral Precipitation from Hydrothermal fluids. Rev. Mineral. 61, 609–631.

Rezvani Khalilabad, M., Axelsson, G., Gíslason, S., 2008. Aquifer characterization with tracer test technique; permanent CO_2 sequestration into basalt, SW Iceland. Mineral. Mag. 72(1), 121–125.

Rimstidt, J. D., 1997. Quartz solubility at low temperatures. Geochim. Cosmochim. Acta 61, 2553–2558.

Rogers, K., Neuhoff, P., Pedersen, A., Bird, D., 2006. CO_2 metasomatism in a basalt hosted petroleum reservoir, Nuussuaq, West-Greenland. Lithos 92, 55–85.

Shock, E., Sassini, D., Willis, M., Sverjensky, D., 1997. Inorganic species in geologic fluids: Correlations among standard molal thermodynamic properties of aqueous ions and hydroxide complexes. Geochim. Cosmochim. Acta 61, 907–950.

Spycher, N., Sonnenthal, E., Zhang, G., Mukhopadyay, S., 2007. Drift-Scale THC Seepage Model. MDL-NBS-HS-000001 REV 05. LBID-2612.

Steefel, C. I., DePaolo, D. J., Lichtner, P. C., 2005. Reactive transport modeling: An essential tool and a new research approach for the Earth sciences. Earth Planet. Sci. Lett. 240, 539–558.

Stefánsson, A., 2001. Dissolution of primary minerals of basalt in natural waters I. Calculation of mineral solubilities from 0°C to 350°C. Chem. Geol. 172, 225–250.

Stefánsson, A., Gíslason, S., 2001. Chemical weathering of basalts, Southwest Iceland: effect of rock crystallinity and secondary minerals on chemical fluxes to the ocean. Am. J. Sci. 301, 513–556.

Stefánsson, A., Gíslason, S., Arnórsson, S., 2001. Dissolution of primary minerals in natural waters II. Mineral saturation state. Chem. Geol. 172, 251–276.

Techer, I., Advocat, T., Lancelot, J., Liotard, J., 2001. Dissolution kinetics of basaltic glasses: control by solution chemistry and protective effect of the alteration film. Chemical Geology 176, 235–263.

Wada, K., Arnalds, O., Kakuto, Y., Wilding, L., Hallmark, C., 1992. Clay minerals of four soils formed in eolian and tephra materials in Iceland. Geoderma 52, 351–365.

Walker, G., 1960. Zeolite zones and dike distribution in relation to the structure of the basalts of eastern Iceland. J. Geol. 68, 515–528.

Wolery, T., 1992. EQ3/6: Software package for geochemical modeling of aqueous systems: Package overview and installation guide (version 7.0). Report UCRL-MA-210662. Lawrence Livermore National Laboratory, Livermore, Calif.

Wolery, T. J., 1983. EQ3NR, A computer program for geochemical aqueous speciation-solubility calculations: Users guide and documentation. UCRL-53414. Lawrence Livermore National Laboratory, Livermore, Calif.

Xu, T., Sonnenthal, E., Spycher, N., Pruess, K., 2006. TOUGHREACT – A simulation program for non-isothermal multiphase reactive geochemical transport in variably saturated geologic media: Applications to geothermal injectivity and CO_2 geologic sequestration. Comput. Geosci. 32, 146–165.

Xu, T., Spycher, N., Sonnenthal, E., Zhang, G., Zheng, L., Pruess, K., 2011. TOUGHREACT Version 2.0: A simulator for subsurface reactive transport under non-isothermal multiphase flow conditions. Comput. Geosci. 37, 763–774.

Table 1: Secondary minerals found in association with basalt alteration (see text for references). Alteration is highly affected by CO_2 concentration.

Basalt weathering, in Iceland[a]	Low temperature (<100°C) geothermal fields, Iceland[a]	Marraat at Nuussuaq, W-Greenland[b]
Amorphous or poorly crystalline Mg, Fe and Al hydroxides, allophane, imogolite, kaolinite and clays	Quartz/chalcedony celadonite, smectite, chlorite, zeolites[c] and calcite	Magnesite, siderite, dolomite, quartz and calcite

[a] CO_2 depleted water-basalt interaction.
[b] CO_2 rich water-basalt interaction.
[c] E.g. analcime, chabazite, thomsonite, scolecite, phillipsite, mesolite, stilbite, stellerite and heulandite.

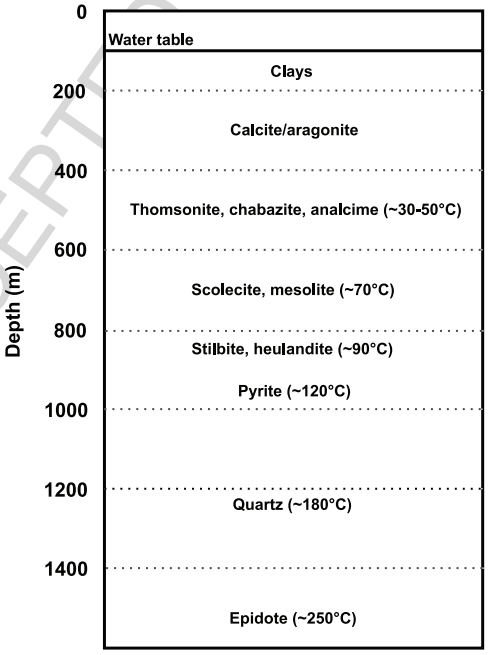

Figure 1: Alteration zones in Hellisheidi along with their approximate depth and temperature range.

Table 2: Chemical composition of the minerals and aqueous species considered in this study.

Group	Mineral	Chemical composition
Aqueous species[a]	$Al(OH)_3$	$Al(OH)_3$
	$Al(OH)_2^+$	$Al(OH)_2^+$
	$Al(OH)^{2+}$	$Al(OH)^{2+}$
	Al^{3+}	Al^{3+}
Primary minerals and glasses	Basaltic glass	$SiAl_{0.36}Fe(II)_{0.19}Mg_{0.28}Ca_{0.26}Na_{0.08}O_{3.31}$
	Plagioclase	$Ca_{0.70}Na_{0.30}Al_{1.70}Si_{2.30}O_8$
	Pyroxene	$Ca_{0.35}Mg_{0.42}Fe_{0.23}SiO_3$
	Olivine	$(Mg_{0.80}Fe_{0.20})_2SiO_4$
Silicates	Allophane	$Al_2O_3(SiO_2)_{1.22}(H_2O)_2.5$
	Amorphous silica	SiO_2
	Antigorite	$Mg_3Si_2O_5(OH)_4$
	Ca-Montmorillonite	$Ca_{0.167}Al_{1.67}Mg_{0.33}Si_4O_{10}(OH)_2$
	Celadonite	$KMgAlSi_4O_{10}(OH)_2$
	Fe-Celadonite	$KFeAlSi_4O_{10}(OH)_2$
	Fe-Chlorite	$Fe_5Al_2Si_3O_{10}(OH)_8$
	Imogolite	$Al_2SiO_3(OH)_4$
	Kaolinite	$Al_2Si_2O_5(OH)_4$
	K-Montmorillonite	$K_{0.33}Al_{1.67}Mg_{0.33}Si_4O_{10}(OH)_2$
	Mg-Chlorite	$Mg_5Al_2Si_3O_{10}(OH)_8$
	Mg-Montmorillonite	$Al_{1.67}Mg_{0.5}Si_4O_{10}(OH)_2$
	Moganite	SiO_2
	Na-Montmorillonite	$Na_{0.33}Al_{1.67}Mg_{0.33}Si_4O_{10}(OH)_2$
	Quartz	SiO_2
Hydroxides	Amorphous Al hydroxide	$Al(OH)_3$
	Fe(II) hydroxide	$Fe(OH)_2$
	Fe(III) hydroxide	$Fe(OH)_3$
Carbonates	Calcite	$CaCO_3$
	Dolomite	$CaMg(CO_3)_2$
	Magnesite	$MgCO_3$
	Siderite	$FeCO_3$
Zeolites	Analcime	$Na_{0.96}Al_{0.96}Si_{2.04}\ O_6 \cdot H_2O$
	Ca-Chabazite	$CaAl_2Si_4O_{12} \cdot 6\ H_2O$
	Ca-Heulandite	$CaAl_2\ Si_7\ O_{18} \cdot 6H_2O$
	Laumontite	$CaAl_2Si_4O_{12} \cdot 4.5\ H_2O$
	Mesolite	$Ca_{0.666}Na_{0.666}Al_2Si_3O_{10} \cdot 2.667\ H_2O$
	Na-Chabazite	$Na_2Al_2Si_4O_{12} \cdot 6\ H_2O$
	Na-Heulandite	$Na_2Al_2Si_7O_{18} \cdot 5\ H_2O$
	Natrolite	$Na_2Al_2Si_3O_{10} \cdot 2\ H_2O$
	Stellerite	$Ca_2Al_4Si_{14}O_{36} \cdot 14\ H_2O$
	Stilbite	$Ca_2NaAl_5Si_{13}O_{36} \cdot 16\ H_2O$

[a] Four Al-hydroxy complexes were added to the EQ3/6 database, which is the primary source of equilibrium constants for aqueous species in this study.

Table 3: Dissociation reactions of the minerals and aqueous species considered in this study.

Group	Mineral	Dissolution reaction
Aqueous species	$Al(OH)_3$	$Al(OH)_3 + H_2O = Al(OH)_4^+ + H^+$
	$Al(OH)_2^+$	$Al(OH)_2^+ + 2\ H_2O = Al(OH)_4^+ + 2\ H^+$
	$Al(OH)^{2+}$	$Al(OH)^{2+} + 3\ H_2O = Al(OH)_4^+ + 3\ H^+$
	Al^{3+}	$Al^{3+} + 4\ H_2O = Al(OH)_4^+ + 4\ H^+$
Primary minerals and glasses	Basaltic glass	$SiAl_{0.36}Fe(II)_{0.19}Mg_{0.28}Ca_{0.26}Na_{0.08}K_{0.008}O_{3.31} + 1.15\ H^+ + 0.14\ H_2O = SiO_{2\,(aq)} + 0.36\ Al(OH)_4^- + 0.19\ Fe^{2+} + 0.28\ Mg^{2+}\ 0.26\ Ca^{2+} + 0.08\ Na^+ + 0.008\ K^+$
	Plagioclase	$Ca_{0.70}Na_{0.30}Al_{1.70}Si_{2.30}O_8 + 3.4\ H_2O = 0.70\ Ca^{2+} + 0.30\ Na^+ + 2.3\ SiO_{2\,(aq)}$
	Pyroxene	$Ca_{0.35}Mg_{0.42}Fe_{0.23}SiO_3 + 2\ H^+ = 0.35\ Ca^{2+} + 0.42\ Mg^{2+} + 0.23\ Fe^{2+} + SiO_{2\,(aq)} + H_2O$
	Olivine	$(Mg_{0.80}Fe_{0.20})_2SiO_4 + 4\ H^+ = 1.60\ Mg^{2+} + 0.40\ Fe^{2+} + SiO_{2\,(aq)} + 2\ H_2O$
Silicates	Allophane	$Al_2O_3(SiO_2)_{1.22}(H_2O)_2.5 + 2.5\ H_2O = 2\ Al(OH)_4^- + 1.22\ SiO_{2\,(aq)} + 2\ H^+$
	Amorphous silica	$SiO_{2\,(am)} = SiO_{2\,(aq)}$
	Antigorite	$Mg_3Si_2O_5(OH)_4 + 6\ H^+ = 3\ Mg^{2+} + 2\ SiO_{2\,(aq)} + 3\ H_2O$
	Ca-Montmorillonite	$Ca_{0.167}Al_{1.67}Mg_{0.33}Si_4O_{10}(OH)_2 + 2.68\ H_2O = 0.165\ Ca^{2+} + 1.67\ Al(OH)_4^- + 0.33\ Mg^{2+} + 4\ SiO_{2\,(aq)} + 0.68\ H^+$
	Celadonite	$KMgAlSi_4O_{10}(OH)_2 + 2\ H^+ = K^+ + Mg^{2+} + Al(OH)_4^- + 4\ SiO_{2\,(aq)}$
	Fe-Celadonite	$KFeAlSi_4O_{10}(OH)_2 + 2\ H^+ + = K^+ + Fe^{2+} + Al(OH)_4^- + 4\ SiO_{2\,(aq)}$
	Fe-Chlorite	$Fe_5Al_2Si_3O_{10}(OH)_8 + 8\ H^+ = 5\ Fe^{2+} + 2\ Al(OH)_4^- + 3\ SiO_{2\,(aq)} + 4\ H_2O$
	Imogolite	$Al_2SiO_3(OH)_4 + 3\ H_2O = 2\ Al(OH)_4^- + SiO_{2\,(aq)} + 2\ H^+$
	Kaolinite	$Al_2Si_2O_5(OH)_4 + 3\ H_2O = 2\ Al(OH)_4^- + 2\ SiO_{2\,(aq)} + 2\ H^+$
	K-Montmorillonite	$K_{0.33}Al_{1.67}Mg_{0.33}Si_4O_{10}(OH)_2 + 2.68\ H_2O = 0.33\ K^+ + 1.67\ Al(OH)_4^- + 0.33\ Mg^{2+} + 4\ SiO_{2\,(aq)} + 0.68\ H^+$
	Mg-Chlorite	$Mg_5Al_2Si_3O_{10}(OH)_8 + 8\ H^+ = 5\ Mg^{2+} + 2\ Al(OH)_4^- + 3\ SiO_{2\,(aq)} + 4\ H_2O$
	Mg-Montmorillonite	$Al_{1.67}Mg_{0.5}Si_4O_{10}(OH)_2 + + 2.68\ H_2O = 0.50\ Mg^{2+} + 1.67\ Al(OH)_4^- + 4\ SiO_{2\,(aq)} + 0.68\ H^+$
	Na-Montmorillonite	$Na_{0.33}Al_{1.67}Mg_{0.33}Si_4O_{10}(OH)_2 + 2.68\ H_2O = 0.33\ Na^+ + 1.67\ Al(OH)_4^- + 0.33\ Mg^{2+} + 4\ SiO_{2\,(aq)} + 0.68\ H^+$
	Quartz	$SiO_2 = SiO_{2\,(aq)}$
Hydroxides	Amorphous Al hydroxide	$Al(OH)_3 + H_2O = Al(OH)_4^- + H^+$
	Fe(II) hydroxide	$Fe(OH)_2\ 2\ H^+ = Fe^{2+} + 2\ H_2O$
	Fe(III) hydroxide	$Fe(OH)_3\ 2\ H^+ = Fe^{2+} + 0.25\ O_{2\,(aq)}\ 2.5\ H_2O$
Carbonates	Calcite	$CaCO_3 + H^+ = Ca^{2+} + HCO_3^-$
	Dolomite	$CaMg(CO_3)_2 + 2\ H^+ = Ca^{2+} + Mg^{2+} + 2\ HCO_3^-$
	Magnesite	$MgCO_3 + H^+ = Mg^{2+} + HCO_3^-$
	Siderite	$FeCO_3 + H^+ = Fe^{2+} + HCO_3^-$
Zeolites	Analcime	$Na_{0.96}Al_{0.96}Si_{2.04}O_6 \cdot\ H_2O + 0.92\ H_2O = 0.96\ Na^+ + 0.96\ Al(OH)_4^- + 2.04\ SiO_{2\,(aq)}$
	Ca-Chabazite	$CaAl_2Si_4O_{12} \cdot\ 6\ H_2O = Ca^{2+} + 2\ Al(OH)_4^- + 4\ SiO_{2\,(aq)} + 2\ H_2O$
	Ca-Heulandite	$CaAl_2\ Si_7\ O_{18} \cdot 6H_2O = Ca^{2+} + 2\ Al(OH)_4^- + 7\ SiO_{2\,(aq)} + 2\ H_2O$
	Laumontite	$CaAl_2Si_4O_{12} \cdot 4.5\ H_2O + 8\ H^+ = Ca^{2+} + 2\ Al^{3+} + 4\ SiO_{2\,(aq)} + 7.5\ H_2O$
	Mesolite	$Ca_{0.67}Na_{0.67}Al_2Si_3O_{10} \cdot\ 2.667\ H_2O + 8\ H^+ = 0.67\ Ca^{2+} + 0.67\ Na^+ + 2\ Al^{3+} + 3\ SiO_{2\,(aq)} + 6.67\ H_2O$
	Na-Chabazite	$Na_2Al_2Si_4O_{12} \cdot\ 6\ H_2O = 2\ Na^+ + 2\ Al(OH)_4^- + 4\ SiO_{2\,(aq)} + 2\ H_2O$
	Na-Heulandite	$Na_2Al_2Si_7O_{18} \cdot 5\ H_2O = 2\ Na^+ + 2\ Al(OH)_4^- + 7\ SiO_{2\,(aq)} + 2\ H_2O$
	Natrolite	$Na_2Al_2Si_3O_{10} \cdot 2\ H_2O + 2\ H_2O = 2\ Na^+ + 2\ Al(OH)_4^- + 3\ SiO_{2\,(aq)}$
	Stellerite	$Ca_2Al_4Si_{14}O_{36} \cdot\ 14\ H_2O = 2\ Ca^{2+} + 4\ Al(OH)_4^- + 14\ SiO_{2\,(aq)} + 6\ H_2O$
	Stilbite	$Ca_2NaAl_5Si_{13}O_{36} \cdot\ 16\ H_2O = 2\ Ca^{2+} + Na^+ + 5\ Al(OH)_4^- + 13\ SiO_{2\,(aq)} + 6\ H_2O$

Table 4: Oxide dissolution reactions and equilibrium constants used for basaltic glass $\log K$ calculations at different temperature.

Oxide	Dissolution reaction	$\log K$ 0° C	$\log K$ 25° C	$\log K$ 60° C	$\log K$ 100° C	$\log K$ 150° C	$\log K$ 200° C	$\log K$ 250° C	$\log K$ 300° C
$SiO_{2\,(am)}$ [a]	$SiO_{2\,(am)} = SiO_{2\,(aq)}$	-2.947	-2.714	-2.445	-2.202	-1.971	-1.802	-1.684	-1.605
Al_2O_3 (Corundum)[b]	$Al_2O_3 + 5\ H_2O = 2\ Al(OH)_4^- + 2\ H^+$	-63.369	-60.908	-58.656	-56.998	-55.809	-55.425	-55.928	-57.757
FeO[b]	$FeO + 2\ H^+ = Fe^{+2} + H_2O$	15.228	13.532	11.580	9.799	8.039	6.626	5.437	4.381
MgO (Periclase)[b]	$MgO + 2\ H^+ = Mg^{+2} + H_2O$	23.742	21.335	18.580	16.082	13.638	11.702	10.101	8.716
CaO (Lime)[b]	$CaO + 2\ H^+ = Ca^{+2} + H_2O$	35.681	32.576	29.011	25.7564	22.545	19.988	17.875	16.058
Na_2O[b]	$Na_2O + 2\ H^+ = 2\ Na^+ + H_2O$	73.075	67.427	60.985	55.166	49.514	45.114	41.587	38.675
K_2O[b]	$K_2O + 2\ H^+ = 2\ K^+ + H_2O$	9.879	84.041	76.192	69.037	62.010	56.474	51.993	48.275

[a] Gunnarsson and Arnórsson (2000)
[b] EQ3/6 database (Wolery, 1992)

Table 5: Dissolution reactions and equilibrium constants for albite, anorthite and chalcedony used for converting SUPCRT dissolution reactions and computed $\log K$ values for analcime, laumontite, Ca-heulandite, stellerite and stilbite to the reactions shown in table 3.

Mineral	Dissolution reaction	$\log K$ 0° C	$\log K$ 25° C	$\log K$ 60° C	$\log K$ 100° C	$\log K$ 150° C	$\log K$ 200° C	$\log K$ 250° C	$\log K$ 300° C
Albite[a]	$NaAlSi_3O_8 + 2\ H_2O = Na^+ + Al(OH)_4^- + 4\ SiO_{2\,(aq)}$	-39.525	-37.301	-35.241	-33.579	-32.098	-31.134	-30.732	-31.177
Anorthite[a]	$CaAl_2Si_2O_8 + 4\ H_2O = Ca^{2+} + 2\ Al(OH)_4^- + 2\ SiO_{2\,(aq)}$	-56.319	-54.579	-53.308	-52.581	-52.297	-52.622	-53.735	-56.186
Chalcedony[b]	$SiO_{2\,(s)} = SiO_{2\,(aq)}$	-3.857	-3.472	-3.106	-2.790	-2.470	-2.205	-1.988	-1.835

[a] Arnórsson and Stefánsson (1999)
[b] EQ3/6 database (Wolery, 1992)

ACCEPTED MANUSCRIPT

Table 6: Standard molar thermodynamic properties for minerals and species considered in this study. $\Delta_f^0 G$ is the Gibbs free energy of formation, $\Delta_f^0 H$ enthalpy of formation, S is the entropy, V the volume (all properties at 1 bar and 298K); a, b and c are the coefficients of the heat capacity polynomial $C_p = a + bT + cT^{-2}$.

Group	Mineral	$\Delta_f^0 G$ kJ/mol	$\Delta_f^0 H$ kJ/mol	S^0 J/mol/K	V^0 cm^3/mol	a J/mol/K	$b \cdot (10^2)$ J/mol/K^2	$c \cdot (10^5)$ J K/mol	$T_{\max}$ ° C	Reference
Aqueous species	$Al(OH)_3$ [a]									
	$Al(OH)_2^+$ [a]									
	$Al(OH)^{2+}$ [a]									
	Al^{3+} [a]									
Primary minerals	Basaltic glass[b]									
and glasses	Plagioclase	-3906.5	-4108.2	217.9	100.8	563.2	-10.875	-0.0033	350	Stefánsson (2001)
	Pyroxene	-2835.3	-2888.5	166.3	65.78	394.7	-4.291	-0.0641	350	Stefánsson (2001)
	Olivine	-1919.7	-2022.9	114.4	44.18	105.09	6.797	-0.1295	350	Stefánsson (2001)
Silicates	Allophane	-3227.90	-3512.22	267						Stefánsson and Gíslason (2001)
	Amorphous silica[c]									
	Antigorite[d]									
	Ca-Montmorillonite[e]									
	Celadonite	-5464.11	-5844.48	287.00	140.4	741.2	-1.8748	-23.688		Holland and Powell (1998)
	Fe-Celadonite	-5127.78	-5497.32	318.00	142.5	756.3	-1.9147	-15.861		Holland and Powell (1998)
	Fe-Chlorite	-6535.56	-7153.99	545.00	213.40	1237.4	1.3594	-37.430		Holland and Powell (1998)
	Imogolite	-2921.80	-3170.38	221						Stefánsson and Gíslason (2001)
	Kaolinite	-3801.72	-4122.33	203.70	99.52	436.7	-3.4295	-40.559		Holland and Powell (1998)
	K-Montmorillonite[e]									
	Mg-Chlorite	-8263.35	-8929.86	410.5	210.9	1161.8	1.0133	-76.573		Holland and Powell (1998)
	Mg-Montmorillonite[e]									
	Moganite[f]	-851.314	-900.723	58.245	22.69[g]	47.00[g]	3.4317[g]	-11.300[g]		Gíslason et al. (1997)
	Na-Montmorillonite[e]									
	Quartz[h]									
Hydroxides	Amorph. Al hydroxide	-1142.23	-1276.12	82.84	31.96				25	Stefánsson and Gíslason (2001)
	Fe(II) hydroxide[e]									
	Fe(III) hydroxide[e]									
Carbonates	Calcite	-1128.81	-1207.54	92.50	36.89	140.9	0.5029	-9.507		Holland and Powell (1998)
	Dolomite	-2161.51	-2324.56	156.00	64.34	305.89	-0.4905	0		Holland and Powell (1998)
	Magnesite	-1027.74	-1111.59	65.10	28.03	186.4	0	0		Holland and Powell (1998)
	Siderite[i]									
Zeolites	Analcime	-3078.89	-3296.9	231.97	97.43	132.5	25.55	-2.13	325	Neuhoff (2000)
	Ca-Chabazite	-7156.38	-7817.83	584.23	247.45	564.18	90.33	-159.2	40	Neuhoff (2000)
	Ca-Heulandite	-9726.32	-10543.79	732.67	319.27	742.54	63.22	-142.79	-70	Neuhoff (2000)
	Laumontite	-6800.52	-7387.49	483.91	209.68	582.22	14.48	-89.94	725	Neuhoff (2000)
	Mesolite	-5505.83	-5940.19	364.97	171.6	201.26	66.05	-20.34	200	Neuhoff (2000)
	Na-Chabazite	-7115.17	-7784.31	619.51	247.45	591.72	91.92	-164.76	40	Neuhoff (2000)
	Na-Heulandite	-9442.15	-10206.77	736.39	314.27	722.37	60.31	-140.11	-70	Neuhoff (2000)
	Natrolite	-5318.31	-5720.06	359.83	169.22	301.40	37.79	-48.63	290	Neuhoff (2000)
	Stellerite	-19929.12	-21661.41	1605.11	666.5	1787.92	63.31	-357.65	230	Fridriksson et al. (2001)
	Stilbite	-20701	-22585.11	1622.94	664.7	1961.68	60.18	-394.39	230	Fridriksson et al. (2001)

[a] logK values for aqueous Al species were calculated using equation 6.
[b] logK values for basaltic glass were calculated using equation 7.
[c] logK values for amorphous silica were calculated using equation 8.
[d] logK values for antigorite were calculated using equation 10.
[e] logK values from the EQ3/6 database (Wolery, 1992).
[f] Moganite molar volume and heat capacity function assumed to be the same as for quartz.
[g] From Helgeson et al. (1978).
[h] logK values for quartz were calculated using equation 9.
[i] logK values for siderite were calculated using equation 11.

Table 7: Equilibrium solubility constants for the dissociation reactions of minerals and aqueous species considered in this study.

Group	Mineral	log K 0° C	log K 25° C	log K 60° C	log K 100° C	log K 150° C	log K 200° C	log K 250° C	log K 300° C
Aqueous species	$Al(OH)_3$	-14.280	-13.203	-11.950	-10.765	-9.552	-8.579	-7.826	-7.322
	$Al(OH)_2^+$	-31.577	-29.842	-28.109	-26.807	-25.916	-25.661	-24.858	-26.874
	$Al(OH)^{2+}$	-37.603	-35.167	-32.615	-30.513	-28.752	-27.738	-27.389	-27.793
	Al^{3+}	-43.426	-40.151	-36.644	-33.614	-30.802	-28.780	-27.439	-26.897
Primary minerals	Basaltic glass	6.697	5.305	3.609	1.995	0.322	-1.121	-2.481	-3.926
and glasses	Plagioclase	-20.14	-18.80	-17.38	-16.46	-15.54	-14.94	-14.62	-14.68
	Pyroxene	11.68	10.45	8.97	7.58	6.23	5.14	4.22	3.38
	Olivine	30.03	26.72	22.91	19.34	15.89	13.15	10.86	8.83
Silicates	Allophane[a]	-72.531	-69.345	-	-	-	-	-	-
	Amorphous silica	-2.947	-2.714	-2.445	-2.202	-1.971	-1.802	-1.684	-1.6050
	Antigorite	37.340	34.485	31.207	28.214	25.268	22.945	21.065	19.514
	Ca-Montmorillonite	-68.299	-64.649	-61.307	-58.714	-56.540	-55.271	-54.945	-55.998
	Celadonite	-34.003	-32.408	-30.951	-29.928	-29.326	-29.365	-30.086	-31.721
	Fe-celadonite	-39.016	-36.989	-35.055	-33.621	-32.641	-32.405	-32.920	-34.399
	Fe-Chlorite	-37.081	-37.959	-39.741	-41.971	-44.927	-48.222	-52.206	-57.541
	Imogolite[a]	-71.820	-68.672	-	-	-	-	-	-
	Kaolinite	-80.765	-76.567	-72.311	-68.822	-65.855	-64.115	-63.586	-64.641
	K-Montmorillonite	-68.767	-64.932	-61.378	-58.587	-56.216	-54.785	-54.322	-55.252
	Mg-Chlorite	-20.662	-23.063	-26.499	-30.120	-34.305	-38.455	-43.044	-48.809
	Mg-Montmorillonite	-68.287	-64.687	-61.402	-58.857	-56.728	-55.490	-55.189	-56.260
	Moganite	-3.035	-2.883	-2.676	-2.469	-2.261	-2.108	-2.010	-1.966
	Na-Montmorillonite	-68.347	-64.593	-61.127	-58.410	-56.102	-54.714	-54.281	-55.232
	Quartz	-4.068	-3.746	-3.355	-2.981	-2.608	-2.325	-2.122	-1.991
Hydroxides	Amorphous Al hydroxide[a]	-32.325	-30.861	-	-	-	-	-	-
	Fe(II) hydroxide	15.341	13.821	12.077	10.491	8.931	7.684	6.635	5.701
	Fe(III) hydroxide	-3.036	-2.832	-2.555	-2.253	-1.910	-1.616	-1.384	-1.224
Carbonates	Calcite	2.285	1.913	1.377	0.770	0.018	-0.752	-1.583	-2.561
	Dolomite	4.286	3.354	2.019	0.524	-1.303	-3.138	-5.073	-7.280
	Magnesite	2.965	2.310	1.423	0.478	-0.625	-1.689	-2.776	-3.978
	Siderite	-0.274	-0.847	-1.554	-2.277	-3.065	-3.715	-4.201	-4.459
Zeolites	Analcime	-34.577	-32.703	-31.029	-29.705	-28.531	-27.772	-27.485	-27.950
	Ca-Chabazite	-70.061	-66.850	-63.599	-60.924	-58.714	-57.609	-57.707	-59.455
	Ca-Heulandite	-68.380	-64.719	-60.907	-57.658	-54.799	-53.102	-52.646	-53.865
	Laumontite	-50.641	-47.889	-44.868	-42.177	-39.671	-37.986	-37.132	-37.308
	Mesolite	-67.155	-64.158	-61.162	-58.700	-56.630	-55.542	-55.548	-57.108
	Na-Chabazite	-68.380	-64.719	-60.907	-57.658	-54.799	-53.102	-52.646	-53.865
	Na-Heulandite	-79.308	-75.060	-70.513	-66.528	-62.892	-60.564	-59.620	-60.488
	Natrolite	-65.657	-62.468	-59.230	-56.512	-54.139	-52.755	-52.461	-53.714
	Stellerite	-67.948	-65.077	-62.195	-59.853	-57.928	-56.984	-57.135	-58.8450
	Stilbite	-190.005	-180.118	-170.786	-163.192	-155.473	-152.258	-150.815	-153.504

[a] Temperature dependence of heat capacity unknown so log K can not be extrapolated to temperature higher than 25°C.

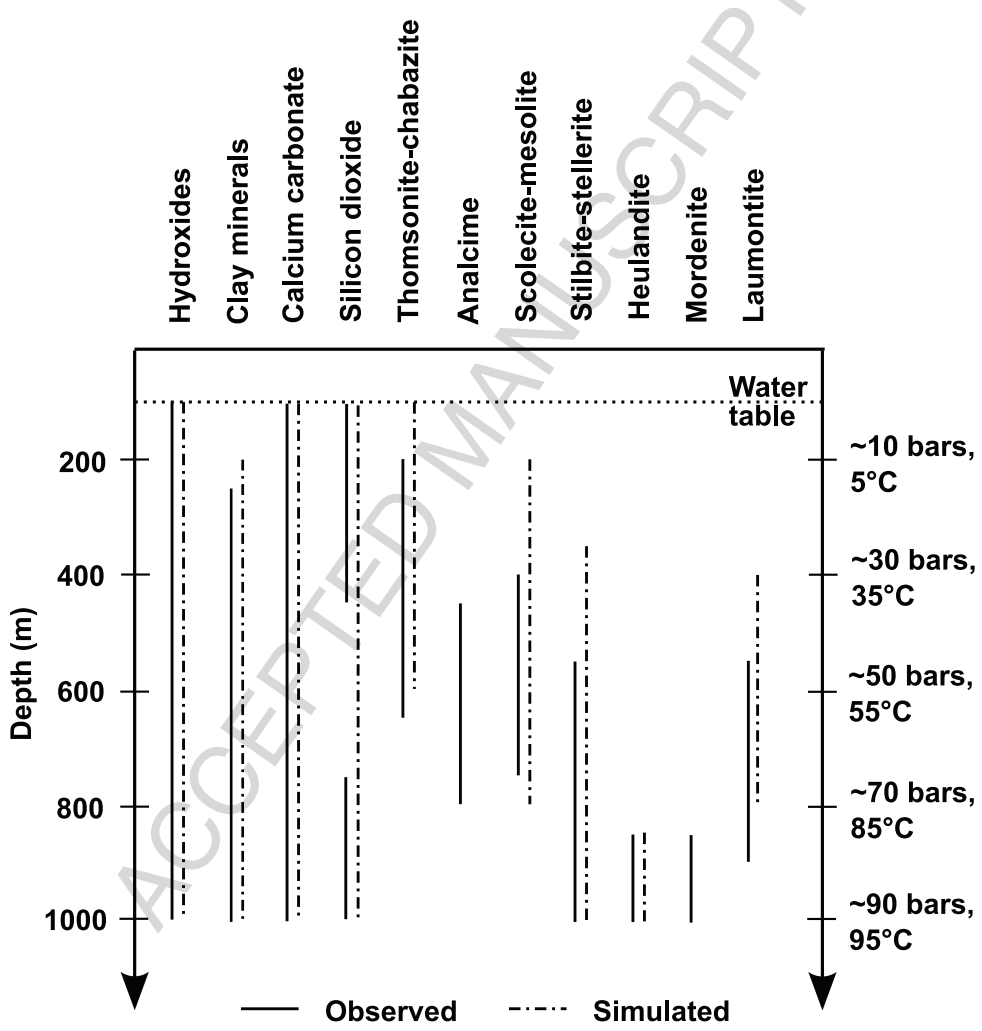

Figure 2: Comparison between observed and simulated basalt alteration under low CO_2 conditions in Hellisheidi. Observed alteration is mainly based on drill cuttings from several wells in the area. Calcium carbonate is either found as calcite or aragonite in Hellisheidi and silicon dioxide as quartz, chalcedony or $SiO_{2\,(am)}$. Thomsonite, scolecite and mordenite were not compiled as potential secondary minerals as the published thermodynamic data for these zeolites resulted in unrealistic results (see text).

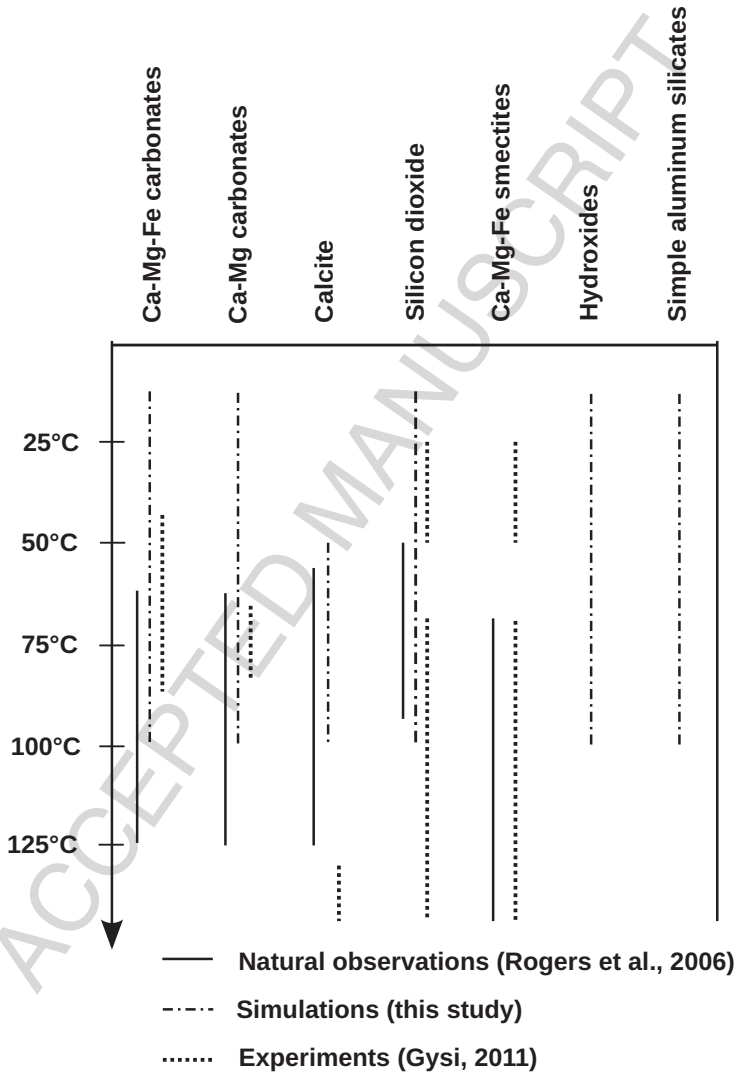

Figure 3: Comparison between simulations, natural observations and laboratory experiments of basalt alteration under elevated CO_2 conditions. Formation of quartz, moganite and/or amorphous SiO_2 is inhibits the uptake of Ca, Mg and Fe into zeolites and clay minerals, which facilitates the formation of calcite, dolomite and magnesite-siderite. Al is removed into hydroxides and simple aluminum silicates. Larger uncertainties are associated with natural temperature (and pressure) conditions than in figure 2, which complicates comparison with alteration as a function of temperature. Good agreement does however exist between overall alteration mineral assemblages observed in Greenland, laboratory experiments and simulations carried out in this study.

Table 8: Initial water[a] (in mmol/L) and primary rock composition (in volume fraction of rock) used in simulations.

Initial water composition		Primary rock composition	
Component	Concentration (mmol/L)	Mineral	Volume fraction of rock
pH/°C	5.70/20	Plagioclase	0.43
CO_2 (DIC)	0.516[b]	Pyroxene	0.39
Si	0.426	Olivine	0.13
Na	0.295	Basaltic glass	0.05
O_2	0.283		
Cl	0.271		
Ca	0.184		
Mg	0.154		
K	0.025		
Fe	0.0002		
Al	0.0001		

[a] Well HK-21, Hellisheidi, Reykjavik Energy database.

[b] CO_2 concentration equaled Henry's law saturation at 10, 20, 30 and 40 bar CO_2 pressure in simulations of water-basalt interaction under elevated CO_2 conditions.

Highlights

- A thermodynamic database describing CO2-water-basalt interaction is presented
- Database validated by comparison to natural alteration at low and elevated CO2 levels
- Import to critically review published data and widely used thermodynamic databases
- Thermodynamic data for numerous important minerals are missing from the literature
- In some cases, published data did not suffice in simulating observed natural alteration